Performance comparison and parametric study on spiral groove gas film face seals

LIU Yuchuan[1], SHEN Xinmin[2], XU Wanfu[3] & WANG Zhili[2]

1. State Key Laboratory of Tribology, Tsinghua University, Beijing 100084, China;
2. School of Mechanical Engineering and Automation, Beijing University of Aeronautics and Astronautics, Beijing 100083, China;
3. Lubrication Technology Research Center, Shenyang Institute of Technology, Shenyang 110015, China

Correspondence should be addressed to Liu Yuchuan (email: liu_yuchuan@263.net)

Received July 1, 2003

Abstract Several spiral groove gas film face seals (SGFS) with different layouts are compared quantitatively to analyze their merits and faults and application behaviors. In addition, a parametric study on downstream mode SGFS is conducted to determine its optimal parameters under certain working conditions. In the computation of gas film pressure on the face, finite element method (FEM) is applied to adapt to complicated geometrical boundary.

Keywords: spiral groove, gas film face seals, parameter study, performance comparison, finite element method.

DOI: 10.1360/ 03yb0239

Gas film face seals (GFFS) have found wide applications in many fluid machines with big power and high rotary speed. For GFFS, on the one hand, compared with tradi-tional contacting mechanical seals, large frictional heat and wear due to high rotary speed are avoided, and on the other hand, leakage is obviously reduced compared with ordinary non-contacting labyrinth seals (about the one tenth of that of labyrinth seals). In addition, by using the bumping effect of typical spiral groove configuration, the seals can achieve zero even negative leakage. In terms of operating principle, GFFS is the round combination of gas lubrication technology and traditional mechanical seals. Since the first spiral groove gas film face seal (SGFS) succeeded on gas pipeline compressor in the 1970s[1], GFFS has been developing steadily. Now GFFS is taking the place of all other type seals in the key locations[2]. One half of studies on GFFS concentrated on the face configuration that decides its performance directly[3]. For the configurations of spi-ral groove the most widespread application have been obtained. In this paper, several SGFS with different layouts are compared quantitatively. And a parametric study on downstream SGFS is developed. These work offers important theoretical foundations for the selection of face configuration and parameter optimization.

1 Theoretical model

The dimensionless steady-state Reynolds equation that describes the gas film pressure for smooth parallel faces is[4]

$$\frac{\partial}{\bar{R}^2\partial\theta}(\bar{H}_0^3\frac{\partial\bar{P}_0^2}{\partial\theta})+\frac{\partial}{\bar{R}\partial\bar{R}}(\bar{R}\bar{H}_0^3\frac{\partial\bar{P}_0^2}{\partial\bar{R}})=2\Lambda\frac{\partial}{\partial\theta}(\bar{P}_0\bar{H}_0). \tag{1}$$

Boundary conditions are

(1) In radial direction, at inner and outer radii, the pressure boundary condition is

$$\bar{P}_0=\bar{P}_i\ (\bar{R}=\bar{R}_i),\quad \bar{P}_0=\bar{P}_o\ (\bar{R}=\bar{R}_o). \tag{2}$$

(2) In circumferential direction, the periodic pressure boundary condition is

$$\bar{P}_0(\theta+2\pi/Z,\bar{R})=\bar{P}_0(\theta,\bar{R}). \tag{3}$$

Introducing transform $\psi=\ln\bar{R}$ and using Galerkin method, we have the variation equation of eq. (1)

$$\iint_\Omega [\bar{H}_0^3\frac{\partial\bar{P}_0^2}{\partial\theta}\frac{\partial\delta\bar{P}_0}{\partial\theta}+\bar{H}_0^3\frac{\partial\bar{P}_0^2}{\partial\psi}\frac{\partial\delta\bar{P}_0}{\partial\psi}-2e^{2\psi}\Lambda\bar{P}_0\bar{H}_0\frac{\partial\delta\bar{P}_0}{\partial\theta}]\mathrm{d}\psi\,\mathrm{d}\theta=0. \tag{4}$$

Discretizing solution domain and coupling Newton-Raphson method with relaxation technique, we have the pressure distribution of gas film. Then the following steady-state behaviors can be obtained through numerical integration and differentiation of pressure.

(1) Dimensionless opening force

$$\bar{F}=\iint_\Omega(\bar{P}_0-1)\bar{R}^2\mathrm{d}\psi\mathrm{d}\theta. \tag{5}$$

(2) Dimensionless film stiffness

$$\bar{K}=-\partial\bar{F}/\partial\bar{H}_0. \tag{6}$$

(3) Dimensionless gas leakage

$$\bar{Q}=-(\int_0^{2\pi}\bar{P}_g\mathrm{d}\theta-2\pi\bar{P}_i)/\ln(\bar{R}_g/\bar{R}_i). \tag{7}$$

(4) Dimensionless power consumption

$$\bar{M}=\iint_\Omega(\frac{\bar{H}_0}{2}\frac{\partial\bar{P}_0}{\partial\theta}\bar{R}^2+\frac{\mathrm{A}}{6\bar{H}_0}\bar{R}^4)\mathrm{d}\psi\mathrm{d}\theta. \tag{8}$$

2 Comparison of steady-state behavior

Shown in fig. 1 are five SGFS in one cycle with different layouts, which have been

treated by the transform $\psi = \ln \overline{R}$ in advance. If high-pressure gas sealed exists at the outer radius, the five layouts are, respectively, downstream bump, upstream dump, herringbone and down-up-stream bump and up-down-stream bump. Their specific structural dimensions and working conditions are shown in table 1. Form the comparisons of their steady-state behaviors shown in fig. 2, we can reach the following conclusions.

(1) Dimensionless opening force versus film thickness

As film thickness increases, opening force decreases. This is the whole trend.

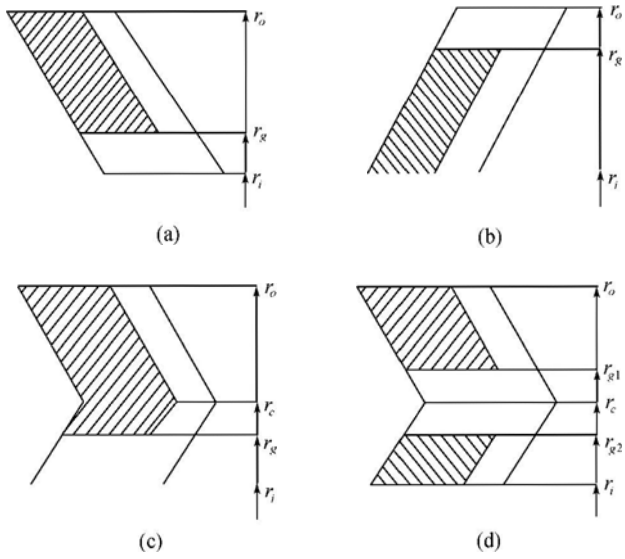

Fig. 1. Layout of different spiral groove faces. (a) Downstream bump; (b) upstream dump; (c) herringbone; (d) down-up-stream bump and up-down-stream bump.

Table 1 Structural dimension and working conditions

Same structural dimension				
Outer radius r_o/m		0.08795	inner radius r_i/m	0.07005
Spiral angle β (°)		72	ratio of groove width to land width w_g/w_l	2.5
Ratio of groove depth to film thickness h_g/h_0		2.25		
Different structural dimension in radial direction				
1	downstream bump	$(r_o - r_g)/(r_g - r_i) = 0.7:0.3$		
2	upstream bump	$(r_o - r_g)/(r_g - r_i) = 0.3:0.7$		
3	herringbone	$(r_o - r_c):(r_c - r_g):(r_g - r_i) = 0.5:0.2:0.3$		
4	down-up-stream bump	$(r_o - r_{g1}):(r_{g1} - r_c):(r_c - r_{g2}):(r_{g2} - r_i) = 0.5:0.15:0.15:0.2$		
5	up-down-stream bump	$(r_o - r_{g1}):(r_{g1} - r_c):(r_c - r_{g2}):(r_{g2} - r_i) = 0.2:0.15:0.15:0.5$		
Same working conditions				
Pressure at outer radius p_o/MPa		0.6	Pressure at inner radius p_i /MPa	0.1
Rotary speed n/rpm		12000	Gas environment temperature T /℃	100

Herringbone has the biggest opening force, while the upstream bump has the smallest. Bigger opening force means stronger capabilty of startup, i.e. sealed face is easy to open at lower rotary speed.

(2) Dimensionless film stiffness versus film thickness

Big film stiffness corresponds to strong tracking capability and anti-perturbation ability. With the decrease in film thickness, this capability will increase. The ranks of the tracking capability, from big to small, are downstream bump, herringbone, down-up-stream bump, up-down-stream bump and upstream dump. The most interesting

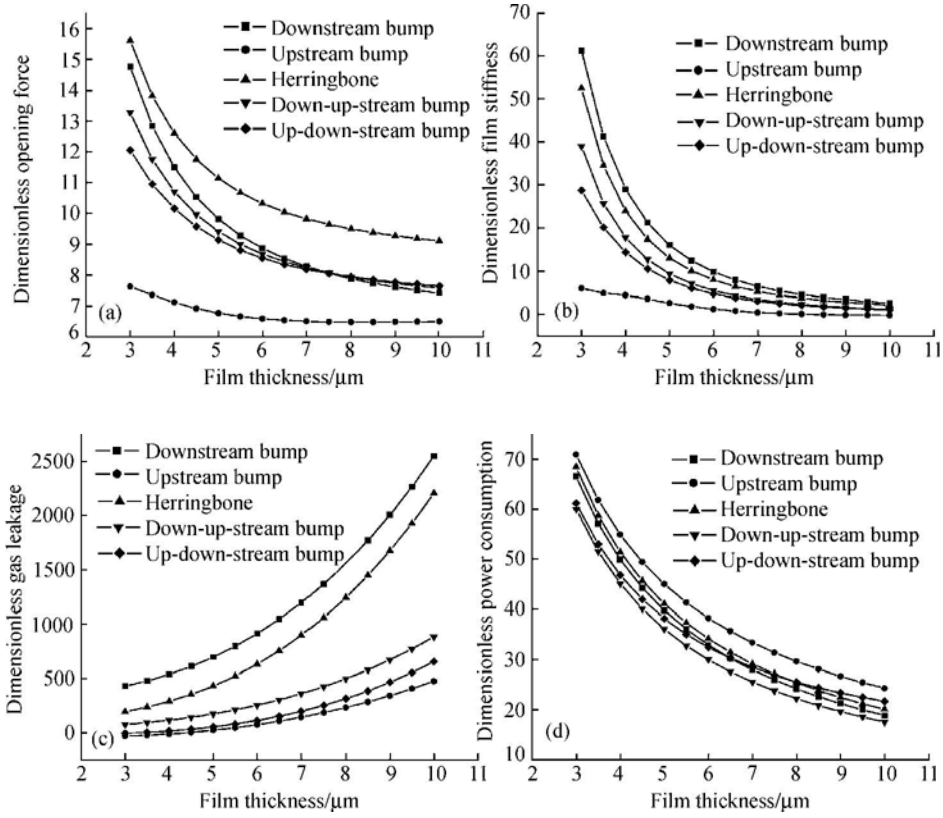

Fig. 2. Comparisons of the steady-state behaviors for five layouts. (a) Dimensionless opening force; (b) dimensionless film stiffness; (c) dimensionless gas leakage; (d) dimensionless power consumption.

thing is that at bigger film thickness the face of upstream bump presents negative stiffness corresponding to film instability.

(3) Dimensionless gas leakage versus film thickness

Big film thickness will cause big leakage. Because the direction of bumping is consistent with that of gas flow from high pressure to low pressure, downstream bump has the biggest leakage while upstream bump has the smallest. In addition, because the bumping effect exceeds the effect of pressure flow, for upstream bump, negative leakage

happens at small film thickness.

(4) Dimensionless power consumption versus film thickness

With the increase in film thickness, the lower effect of viscous shear will decrease the power consumption, which is the general tendency as shown in fig. 2(d). At the same film thickness, the upstream bump has the biggest power consumption, while down-up-stream bump has the smallest.

3 Parametric study

For the most widely used downstream spiral groove face configuration, the influ-ences of structural parameters, such as spiral angle, groove number, ratio of groove width to land width, groove radius, and groove depth, on the seal behaviors are investigated (figs. 3—7). The parametric study is conducted around a specific parameter point, i.e. r_o=0.08795(m), r_i=0.07005(m), r_g=0.07875(m), β =75(deg), w_g/w_l=1.0, h_g=5(μm), h_0=5.6(μm). The working condition is the same in table 1 while the variable ranges of the above structural parameters are shown in table 2. From the comparisons, the following conclusions were drawn:

Table 2 The variable range of structural parameters

Fig. 3 spiral angle β (deg)	10—80
Fig. 4 groove number z	5—50
Fig. 5 ratio of groove width to land width w_g/w_l	0.25—5
Fig. 6 groove radius r_g/m	0.071—0.087
Fig. 7 groove depth h_g/um	2—20

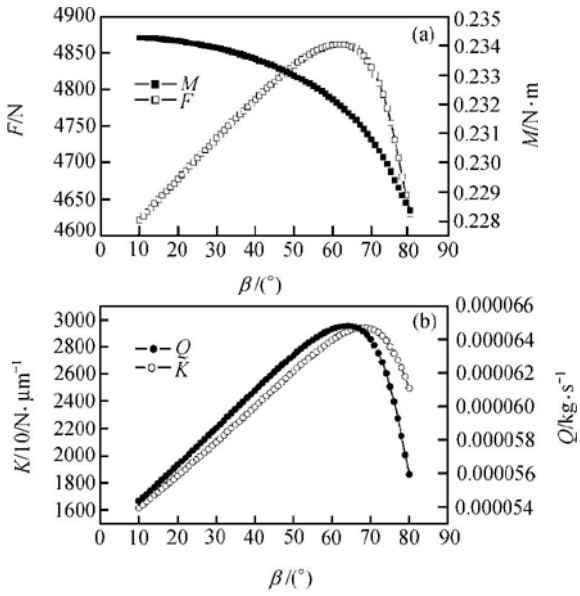

Fig. 3. The influence of spiral angle on opening force and power consumption (a) and film stiffness and gas leak-age (b).

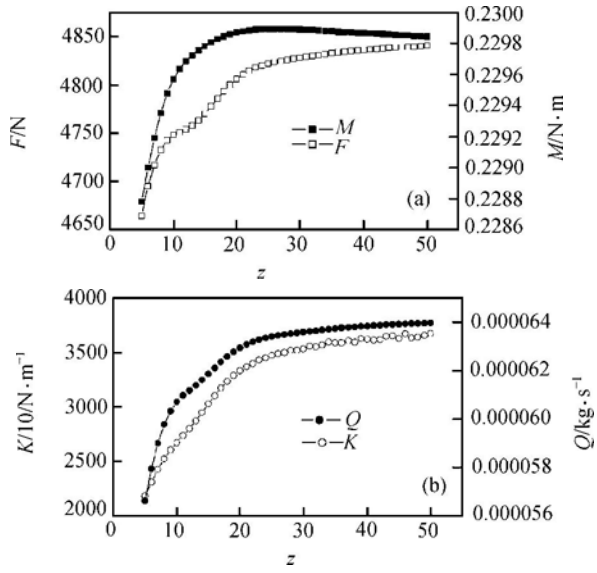

Fig. 4. The influence of groove number on opening force and power consumption (a) and film stiffness and gas leakage (b).

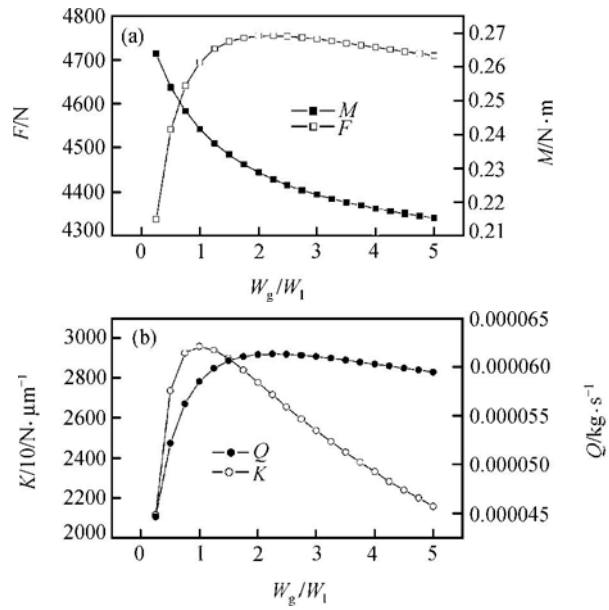

Fig. 5. The influence of ratio of groove width to land width on opening force and power consumption (a) and film stiffness and gas leakage (b).

The optimum parameters for maximum film stiffness are: $(r_o-r_g)/(r_g-r_i)=2.0$, β = 67(deg), $w_g/w_l=1.0$, and $h_g/h_0=1.0$, while the optimum parameters for maximum opening force are: $(r_o-r_g)/(r_g-r_i)=2.0$, β =62(deg), $w_g/w_l=2.0$, $h_g/h_0=2.0$. As shown in fig. 4, when

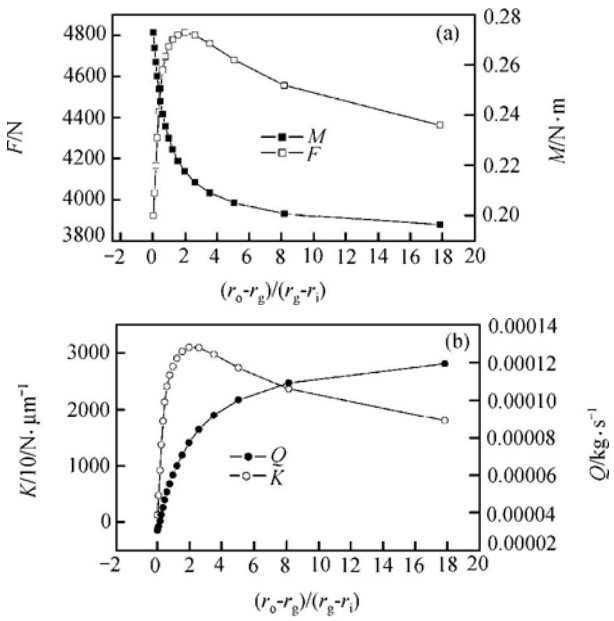

Fig. 6. The influence of ratio of groove radius on opening force and power consumption (a); and film stiffness and gas leakage (b).

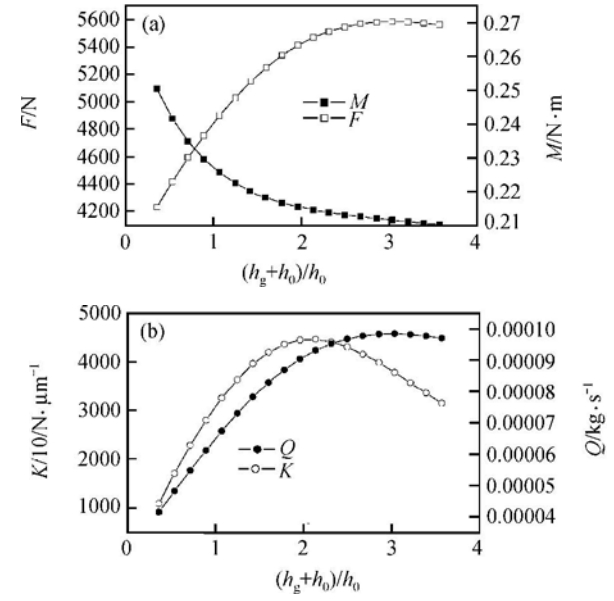

Fig. 7. The influence of groove depth on opening force and power consumption (a); and film stiffness and gas leakage (b).

groove number exceeds 30, the seal performances do not change. The above optimal results accord with similar analyses of gas seals[5,6] and gas bearings[7].

4 Conclusion

In this paper several SGFS with different layouts are compared quantitatively. And a parametric study on downstream SGFS is conducted to obtain the optimum parameters for specific running condition. This work lays a theoretical foundation for the selection of face configuration and parameter optimization.

References

1. Netzel, J. P., High performance gas compressor seals, in Proceedings of the 11th International Conference on Fluid Sealing, Cannes, 1987 (ed. Nau, B. S.), London: Elsevier Applied Science Publishers, 1987, 532—547.
2. Pecht, G. G., Netzel, J. P., Design and application of non-contacting gas lubricated seals for slow speed ser-vices, Lubrication Engineering, 1999, 55 (7): 20—25.
3. Sedy, J., Improved performance of film-riding gas seals through enhancement of hydrodynamic effects, ASLE Trans., 1980, 23 (1): 35—44.
4. Liu Y., Shen, X., Xu, W., Numerical analysis of dynamic coefficients for gas film face seals, ASME J. of Tribology, 2002, 124 (4): 743—754.[DOI]
5. Zirkelback, N., Parametric study of spiral groove gas face seals, Tribology Trans., 2000, 43 (2): 337—343.
6. Gu, Y., Mechanical Face Seals, Dongying: Beijing University of Petroleum Press, 1994, 174—184.
7. Wang, Y., Gas Lubricated Theory and Design Manual of Gas Bearings, Beijing, China Machine Press, 1999, 96—117.